Bubble kicks for primordial black holes to form more binaries

Zi-Yan Yuwen (宇文子炎)

ITP, CAS

June 28th, 2024

Based on recent work 2406.05838 collaborative with
Cristian Joana, Shao-Jiang Wang, Rong-Gen Cai

Cosmological first-order phase transition (FOPT) [1, 2, 3, 4] is a possible phenomenon in the early universe to go beyond the Standard Model and to probe new physics with associated productions of stochastic gravitational-wave backgrounds (SGWBs) [5, 6]. The energy scale for a FOPT ranges widely from inflation to QCD phase transitions.

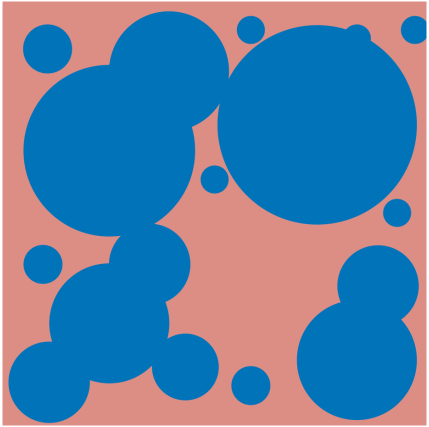

Figure 1: Vacuum bubbles and cosmological first-order phase trnasitions.

Primordial black hole collapsing

Primordial black holes (PBHs) can naturally arise from many scenarios [7, 8, 9, 10]. The quantum fluctuations during inflation rapidly froze because of the shrinking of the comoving Hubble horizons, which resulted in classical over-dense regions. The energy scale for a PBH formation mechanism ranges widely from inflation to BBN and even later.

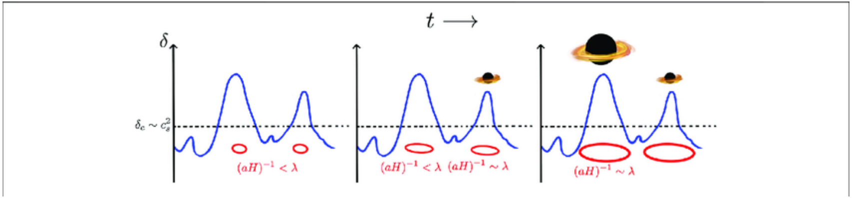

Figure 2: Sketch of PBH formations [11]

It does not seem interesting to have a FOPT happen first and then PBH forms, where the universe has settled down in the true vacuum.

What if to have PBH formations first and then an FOPT happens? The former's works have analyzed how the existing PBHs affect the nucleation rates [12, 13] [1] (where I still have some doubts) of vacuum bubbles, and the possible subsequent phenomenon [14, 15] [2] based on the conclusions on nucleation rates.

---

[1] Philipp Burda, Ruth Gregory, and Ian Moss. "Vacuum metastability with black holes", and Kyohei Mukaida and Masaki Yamada. "False Vacuum Decay Catalyzed by Black Holes".

[2] Zhen-Min Zeng and Zong-Kuan Guo. "Phase transition catalyzed by primordial black holes", and Ryusuke Jinno, Jun'ya Kume, and Masaki Yamada. "Super-slow phase transition catalyzed by BHs and the birth of baby BHs".

What about the interactions between the black holes and the bubbles? A Numerical Relativity simulation is needed!

Since the width of the bubble wall shrinks when expanding, mesh refinement is required in the simulation.

We use GRChombo[16, 17], a AMR based open-source code for numerical relativity simulations.

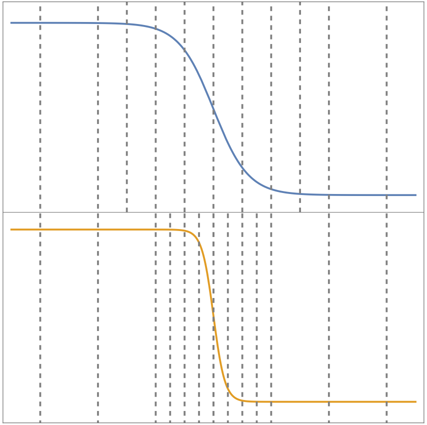

Figure 3: AMR applied on scalar bubble

We consider a universe with a black hole suffering FOPT, which is described by a real scalar field,

$$S = \int \mathrm{d}^4x\sqrt{-g}\left(\frac{1}{M_{\mathrm{pl}}^2}R - \frac{1}{2}g^{\mu\nu}\partial_\mu\phi\partial_\nu\phi - V(\phi)\right), \tag{1}$$

where the potential for the scalar field reads

$$V(\phi) = \left(1 + a\left(\frac{\phi}{\phi_0}\right)^2 - (2a-4)\left(\frac{\phi}{\phi_0}\right)^3 + (a+3)\left(\frac{\phi}{\phi_0}\right)^4\right)(V_F - V_T) + V_T. \tag{2}$$

This potential has a local minimum V_F at $\phi = 0$ and a global minimum V_T at $\phi = \phi_0$, corresponding to the false vacuum and true vacuum respectively.

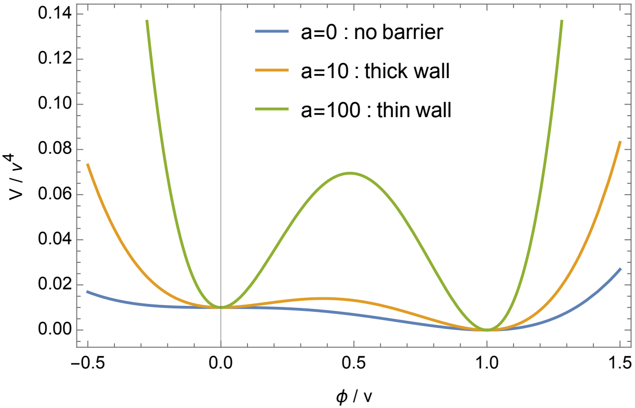

Figure 4: Potential for several possible parameters

Initial data

The initial scalar field profile takes the following ansatz,

$$\phi_{\mathrm{i}}(r)=\frac{\phi_0}{2}\left(1-\tanh\left(\frac{r-r_0}{D_0}\right)\right), \quad \dot{\phi}_{\mathrm{i}}(r)=0, \tag{3}$$

where r_0 and D_0 are the radius and width of the bubble respectively.

Besides the vacuum bubble, a PBH is assumed to exist and stay in the false vacuum, where the universe is dominated by the potential V_F.

Let M be the length scale in the simulation. $c = G = \hbar = 1$.

- Effectively box size $128M \times 128M \times 128M$ with periodic boudary conditons.
- Mass of PBH $m_{\rm PBH} = 0.502M$, which is arrived by setting $m_{\rm PBH,i} = 0.5M$ and solving the Hamiltonian and Momentum Constraints.
- Separation between PBH and bubble $40M$.
- Other parameters are set to be $V_F = 10^{-5}M^{-4}$, $V_T = 0$, $\phi_0 = 0.01M$, $a = 10$, $r_0 = 3M$, and $D_0 = 15M$, respectively.

Periodic boundary conditions along x-direction, reflective boudary conditions along y and z directions.

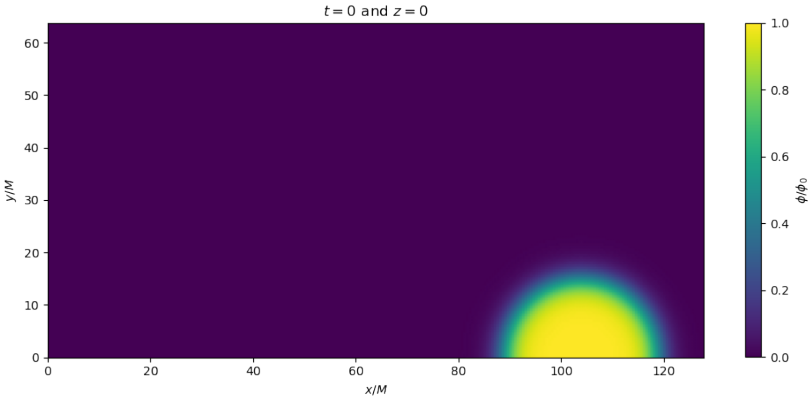

Figure 5: Initial configuration for the scalar field

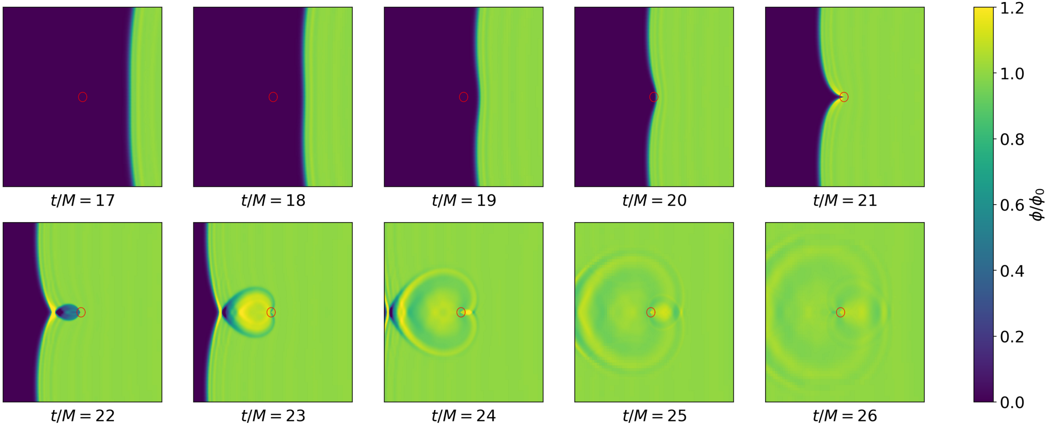

Figure 6: Scalar field profile when the vacuum bubble crosses the PBH at around $t = 20M$, whose apparent horizon is painted in red circles.

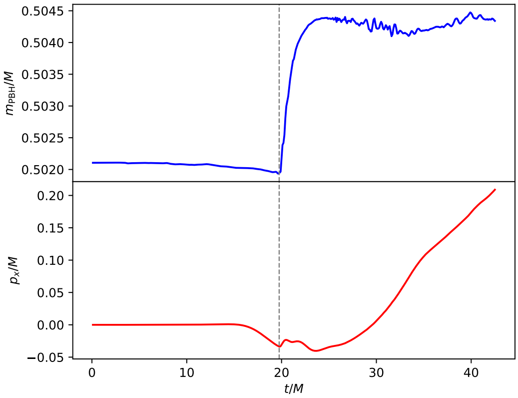

Figure 7: The time evolution for the PBH mass $m_{\rm PBH}$ and momentum along x-direction p_x. The gray dashed line denotes the collision time for the vacuum bubble and the PBH.

- The PBH extracts energy from the bubble wall, leading to a mass enhancement by about 0.5%. This phenomenon is expected to be more significant for a late time expansion when the energy density on the bubble wall is large.
- The strong collision with the scalar field brings momentum to the PBH. An interesting phenomenon is that the bubble does not push the black hole away, but rather pulls it towards the center of the bubble.
- Interactions between the PBH and the scalar field disrupts the spherical symmetry of the bubble wall, which leads to GW radiation both from the bubble and from the PBH. The scalar field oscillates at length scale comparable to the radius of the PBH, which corresponds to a high-frequency GW radiation.

However, it is difficult to obtain a good definition of GWs in a non-asymptotically flat spacetime background with an unbounded matter distribution. Thus the GW radiations are expected to exist but are hard to extract ...

Let us focus on the second phenomenon which modifies the binary formation rate for the PBHs. For PBHs with masses $m_{\rm PBH}$ separated by a comoving distance x, the decoupling happens if $m_{\rm PBH} \cdot (ax)^{-3} > \rho$, where ρ is the energy density of the background cosmic fluid [18, 19], which can not be satisfied in radiation-dominated epoch. In matter-dominated epoch, the condition for forming a binary would be

$$f \cdot \left(\frac{\bar{x}}{x}\right)^3 > 1. \tag{4}$$

The average comoving distance $\bar{x}$ could be estimated from the definition of f at matter-radiation equality,

$$f = \frac{m_{\rm PBH}}{\frac{4\pi}{3}(a_{\rm eq}\bar{x})^3}\left(\frac{1}{2}\frac{3H_{\rm eq}^2}{8\pi G}\right)^{-1} = \frac{2\gamma H_{\rm PBH}^{-1} H_{\rm eq}^{-2}}{(a_{\rm eq}\bar{x})^3}. \tag{5}$$

Assuming the neighboring PBHs' distances are homogeneously distributed in the interval $(0, x_{\max})$, where $x_{\max} = 4\bar{x}/3$ to keep $\bar{x}$ the average distance. For PBHs with almost no initial velocity, the possibility for two PBHs forming a binary as

$$P_0 = \frac{f\bar{x}^3}{x_{\max}^3} = \frac{27}{64}f. \tag{6}$$

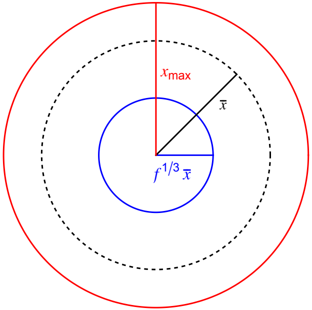

Figure 8: Distribution region of a neighboring PBH.

However, from the simulation above, a PBH near a vacuum bubble gains a velocity during FOPT. Assuming the velocities share the same norm V but randomly distributed in directions. Then the relative velocity of two PBHs is uniformly distributed from 0 to $2V$, the average of which is V.

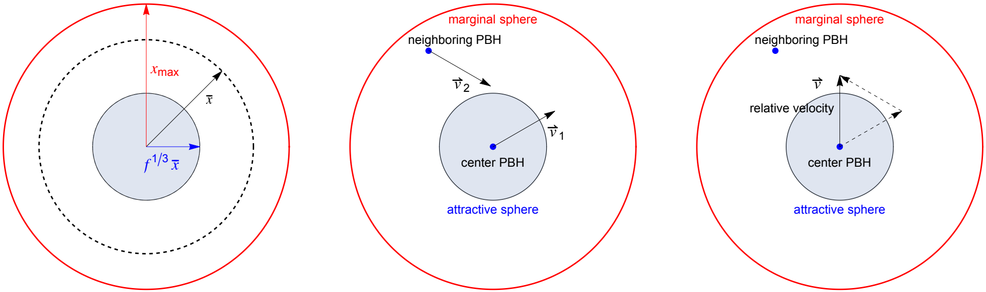

(a) Initial case (b) PBHs gain velocity (c) Relative velocity

Figure 9: How velocity modifies the binary formation criterion.

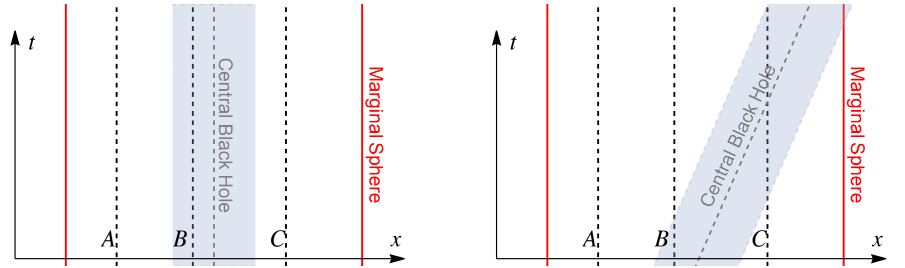

(a) Black holes with no velocities

(b) The central black hole moves with an relative velocity

Figure 10: An $1+1$ dimensional view of how the relative velocity gained by the central PBH modifies the decoupling region.

After the phase transition, the evolution of the universe is described by a radiation-dominated FLRW universe with $\mathrm{d}s^2 = -\mathrm{d}t^2 + a^2\mathrm{d}\mathbf{x}^2$, where the PBHs can be regarded as massive particles. Solving the geodesic equations gives out the 4-velocity

$$u^\mu := \frac{\mathrm{d}x^\mu}{\mathrm{d}\tau} = \left(\sqrt{\frac{(a_{\mathrm{PT}}v)^2}{(a/a_{\mathrm{PT}})^2} + 1}, \frac{v}{(a/a_{\mathrm{PT}})^2}, 0, 0\right), \tag{7}$$

where a_{PT} is the scale factor at phase transition, and v is a constant. The dimensionless combination $a_{\mathrm{PT}}v$ can be interpreted as the "velocity" of the PBH if $1/\sqrt{1-(a_{\mathrm{PT}}v)^2} \sim O(1)$. The frictions from cosmic fluid are neglected.

Since the matter-dominated epoch takes over the age of the universe, the comoving distance moved by a massive particle with velocity v from matter-radiation equality t_{eq} to nowadays t_0 is

$$\begin{aligned}\Delta x &= \int_{t_{\mathrm{eq}}}^{t_0} \mathrm{d}t \frac{\mathrm{d}x}{\mathrm{d}t} \simeq v t_{\mathrm{eq}} \int_{t_{\mathrm{eq}}}^{t_0} \frac{\mathrm{d}(t/t_{\mathrm{eq}})}{(a/a_{\mathrm{PT}})^2} \\ &= \frac{v}{2H_{\mathrm{eq}}} \int_{a_{\mathrm{eq}}}^{a_0} \frac{3}{2} \left(\frac{a}{a_{\mathrm{eq}}^3}\right)^{1/2} \left(\frac{a_{\mathrm{PT}}}{a}\right)^2 \mathrm{d}a \simeq \frac{3v}{2H_{\mathrm{eq}}} \left(\frac{a_{\mathrm{PT}}}{a_{\mathrm{eq}}}\right)^2 .\end{aligned} \tag{8}$$

In the last line, we dropped a term contributed by a_0 since $a_0 \gg a_{\mathrm{eq}}$.

Comparing Δx with $\bar{x}$ gives a clear picture of how far a PBH moves,

$$\frac{\Delta x}{\bar{x}} = \frac{3}{2}(a_{\rm PT}v)\left(\frac{f}{2\gamma}\right)^{1/3}\left(\frac{a_{\rm eq}}{a_{\rm PBH}}\right)^{2/3}\left(\frac{a_{\rm PT}}{a_{\rm eq}}\right) \equiv \Gamma f^{1/3}. \tag{9}$$

For QCD phase transition $a_{\rm PT}/a_{\rm eq} \simeq 10^8$, PBHs formed before EW scale $a_{\rm PBH}/a_{\rm eq} \simeq 10^{12}$ with efficiency $\gamma = 0.2$ and velocity $a_{\rm PT}v = 0.3$, one obtains a rough estimation $\Gamma \sim O(1)$ and $\Delta x \simeq f^{1/3}\bar{x}$.

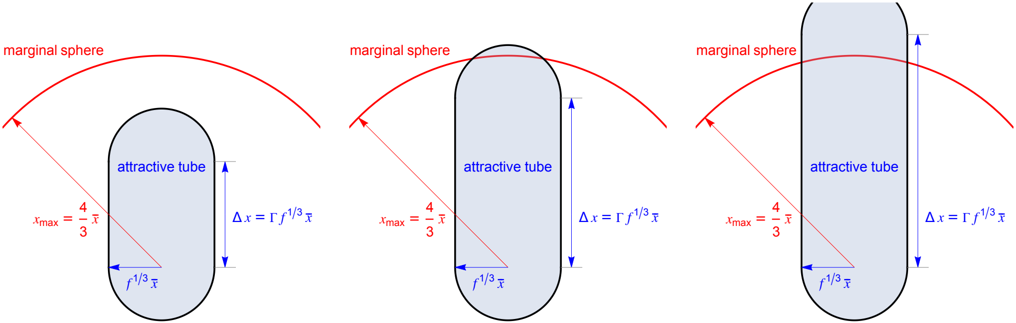

(a) $f^{1/3} < \frac{4}{3}(\Gamma+1)^{-1}$ (b) $\frac{4}{3}(\Gamma+1)^{-1} < f^{1/3} < \frac{4}{3}(\Gamma^2+1)^{-1/2}$ (c) $f^{1/3} > \frac{4}{3}(\Gamma^2+1)^{-1/2}$

Figure 11: Three situations of the relation between the attractive tube and the marginal sphere.

The simplest case is when $f^{1/3} < \frac{4}{3}(\Gamma+1)^{-1}$, the attractive tube does not reach the marginal sphere, as is shown in the left panel of Fig. 11(a). The probability is given by the ratio of the volume of the attractive tube to that of the marginal sphere,

$$P = \left(\frac{4\pi}{3} f\bar{x}^3 + \pi\Gamma f\bar{x}^3\right) \Big/ \left(\frac{4\pi}{3} x_{\max}^3\right) = \frac{27(4+3\Gamma)}{256} f. \tag{10}$$

When $f^{1/3} > \frac{4}{3}(\Gamma^2+1)^{-1/2}$, it is also easy to evaluate the possibility, since the attractive tube extends far outside the marginal sphere, as shown in the right panel of Fig. 11(c). The possibility now reads

$$\begin{aligned} P =& \left(\frac{2\pi}{3} f \bar{x}^3 + \frac{2}{3}\pi f^{2/3}\sqrt{\frac{16}{9} - f^{2/3}}\bar{x}^3 + \frac{2\pi}{3}(1-\cos\theta)x_{\max}^3\right) \Bigg/ \left(\frac{4\pi}{3}x_{\max}^3\right) \\ =& \frac{27}{128}\left(f + f^{2/3}\sqrt{\frac{16}{9} - f^{2/3}}\right) + \frac{1-\cos\theta}{2}, \end{aligned} \tag{11}$$

where the angle θ is given by

$$\theta = \arcsin\left(\frac{3}{4}f^{1/3}\right). \tag{12}$$

As for the third case with $\frac{4}{3}(\Gamma+1)^{-1} < f^{1/3} < \frac{4}{3}(\Gamma^2+1)^{-1/2}$, the calculation is more complicated but still straightforward and less important, which is shown in the middle panel of Fig. 11(b). The main idea is to calculate the ratio of the attractive tube inside the marginal sphere to the total volume.

$$P = \frac{27}{256}\left(2+3\Gamma-2\cos\theta_1\right) f + \frac{\cos\theta_2 - 1}{2} + \frac{\sin^2\theta_2\cos\theta_1}{4}\left(\frac{3f^{1/3}\cos\theta_1}{4\cos\theta_2} - 1\right), \tag{13}$$

where

$$\theta_1 = \pi - \arccos\left(\frac{(\Gamma^2+1)f^{2/3} - \frac{16}{9}}{2\Gamma f^{2/3}}\right), \quad \theta_2 = \arccos\left(\frac{\frac{16}{9} + (\Gamma^2-1)f^{2/3}}{\frac{8}{3}\Gamma f^{1/3}}\right). \tag{14}$$

Taking $\Gamma = 1$ as an example, the ratio of the modified possibility P to the original one P_0 is given by

$$\frac{P}{P_0} = \begin{cases} \dfrac{7}{4}\,, & f < \dfrac{8}{27} \\ \dfrac{1}{2} + \dfrac{64 - \left(16 - 9f^{2/3}\right)^{3/2}}{54f}\,, & \dfrac{8}{27} < f < \dfrac{16\sqrt{2}}{27} \\ \dfrac{4}{3} + \dfrac{32}{27f} - \dfrac{16}{27f^{4/3}}\,, & \dfrac{16\sqrt{2}}{27} < f < 1 \end{cases}. \tag{15}$$

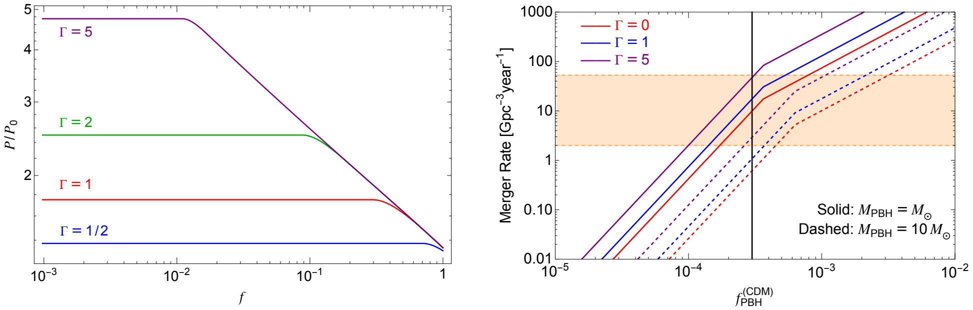

Figure 12: Left: The ratios P/P_0 for different Γ. The ratio returns to 1 as $\Gamma \to 0$ corresponding to $v = 0$. Right: Modified merger rate as a function of $f_{\mathrm{PBH}}^{(\mathrm{CDM})} = f\Omega_{\mathrm{m}}/\Omega_{\mathrm{CDM}}$. The horizontal shaded region in orange is the LIGO-Virgo constraint on the event rate $2 \sim 53\ \mathrm{Gpc}^{-3}\mathrm{year}^{-1}$ [20], while the vertical black line at $f_{\mathrm{PBH}}^{(\mathrm{CDM})} \simeq 3 \times 10^{-4}$ is the upper limit from non-detection of CMB distortion [21].

Simulation

Three phenomena:

- Mass enhancement. Depending on the separation and mass of the black hole.
- GW radiation. May be related to the QNMs of the black hole.
- Momentum transfer. May be more significant for a lighter black hole.

The simulation can not last for a longer time for the following two reasons.

- There is no dissipative effect in the system, thus the scalar field will never settle down at the true vacuum but finally oscillate with a very small length scale, which is numerically unstable and would diverge when the mesh refinement rate can not keep up with the oscillations.
- The “moving punctures” gauge does not work well after a black hole suffers a “phase transition” (from asymptotically de Sitter to asymptotically flat).

Initially, the shift vector pulls observers away from the center of the black hole to avoid falling into the central singularity, and to overcome the inflation of the background. Since the collision time is short, the black hole suddenly transfers to an asymptotically flat one. This process happens too quickly for the observers to slow down, which leads to a continually shrinking coordinate radius of the apparent horizon and increases numerical errors.

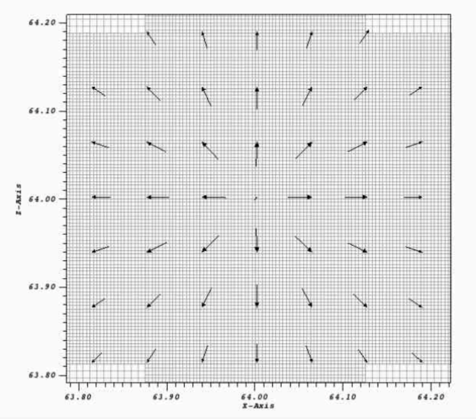

Figure 13: Shift vectors in Moving puncture gauge [22].

Modified binary formation rates

There are several basic assumptions in the estimation:

- Uniformly distribution of PBHs with no clustering. Results may be dramatically changed if PBHs are clustered, which is more difficult to consider.
- Monochromatic PBHs are considered, so that the velocities are assumed to be the same.

Further studies

- How to find a better gauge choice for a black hole suffering “phase transition”?
- How to extract the GWs for such a non-asymptotically flat and unbound gravitational system?
- Add radiation-like matter?

Thanks!

[1] Anupam Mazumdar and Graham White.
Review of cosmic phase transitions: their significance and experimental signatures.
Rept. Prog. Phys., 82(7):076901, 2019.

[2] Mark B. Hindmarsh, Marvin Lüben, Johannes Lumma, and Martin Pauly.
Phase transitions in the early universe.
SciPost Phys. Lect. Notes, 24:1, 2021.

[3] Robert Caldwell et al.
Detection of early-universe gravitational-wave signatures and fundamental physics.
Gen. Rel. Grav., 54(12):156, 2022.

[4] Peter Athron, Csaba Balázs, Andrew Fowlie, Lachlan Morris, and Lei Wu.
Cosmological phase transitions: From perturbative particle physics to gravitational waves.
Prog. Part. Nucl. Phys., 135:104094, 2024.

[5] Chiara Caprini et al.
Science with the space-based interferometer eLISA. II: Gravitational waves from cosmological phase transitions.
JCAP, 1604:001, 2016.

[6] Chiara Caprini et al.
Detecting gravitational waves from cosmological phase transitions with LISA: an update.
JCAP, 2003:024, 2020.

[7] Bernard J. Carr and James E. Lidsey.
Primordial black holes and generalized constraints on chaotic inflation.
Phys. Rev. D, 48:543–553, 1993.

[8] P. Ivanov, P. Naselsky, and I. Novikov.
Inflation and primordial black holes as dark matter.
Phys. Rev. D, 50:7173–7178, 1994.

[9] Lisa Randall, Marin Soljacic, and Alan H. Guth.
Supernatural inflation: Inflation from supersymmetry with no (very) small parameters.
Nucl. Phys. B, 472:377–408, 1996.

[10] Pisin Chen.
Inflation induced Planck-size black hole remnants as dark matter.
New Astron. Rev., 49:233–239, 2005.

[11] Pablo Villanueva-Domingo, Olga Mena, and Sergio Palomares-Ruiz.
A brief review on primordial black holes as dark matter.
Front. Astron. Space Sci., 8:87, 2021.

[12] Philipp Burda, Ruth Gregory, and Ian Moss.
Vacuum metastability with black holes.
JHEP, 08:114, 2015.

[13] Kyohei Mukaida and Masaki Yamada.
False Vacuum Decay Catalyzed by Black Holes.
Phys. Rev. D, 96(10):103514, 2017.

[14] Zhen-Min Zeng and Zong-Kuan Guo.
Phase transition catalyzed by primordial black holes.
2 2024.

[15] Ryusuke Jinno, Jun'ya Kume, and Masaki Yamada.
Super-slow phase transition catalyzed by BHs and the birth of baby BHs.
Phys. Lett. B, 849:138465, 2024.

[16] Katy Clough, Pau Figueras, Hal Finkel, Markus Kunesch, Eugene A. Lim, and Saran Tunyasuvunakool.
GRChombo : Numerical Relativity with Adaptive Mesh Refinement.
Class. Quant. Grav., 32(24):245011, 2015.

[17] Tomas Andrade et al.
GRChombo: An adaptable numerical relativity code for fundamental physics.
J. Open Source Softw., 6(68):3703, 2021.

[18] Misao Sasaki, Teruaki Suyama, Takahiro Tanaka, and Shuichiro Yokoyama.
Primordial Black Hole Scenario for the Gravitational-Wave Event GW150914.
Phys. Rev. Lett., 117(6):061101, 2016.
[Erratum: Phys.Rev.Lett. 121, 059901 (2018)].

[19] V. De Luca, G. Franciolini, P. Pani, and A. Riotto.
The evolution of primordial black holes and their final observable spins.
JCAP, 04:052, 2020.

[20] B. P. Abbott et al.
The Rate of Binary Black Hole Mergers Inferred from Advanced LIGO Observations Surrounding GW150914.
Astrophys. J. Lett., 833(1):L1, 2016.

[21] Massimo Ricotti, Jeremiah P. Ostriker, and Katherine J. Mack.
Effect of Primordial Black Holes on the Cosmic Microwave Background and Cosmological Parameter Estimates.
Astrophys. J., 680:829, 2008.

[22] Katy Clough.
Scalar Fields in Numerical General Relativity: Inhomogeneous inflation and asymmetric bubble collapse.
PhD thesis, King's Coll. London, Cham, 2017.